Microsyst Technol
DOI 10.1007/s00542-015-2471-1

TECHNICAL PAPER

Design and performance evaluation of a biomimetic microrobot for the father–son underwater intervention robotic system

Chunfeng Yue · Shuxiang Guo · Liwei Shi

Received: 12 January 2015 / Accepted: 30 January 2015
© Springer-Verlag Berlin Heidelberg 2015

Abstract Underwater intervention is a favorite and difficult task for AUVs. To realize the underwater manipulation for the small size spherical underwater robot SUR-II, a father–son underwater intervention robotic system (FUIRS) is proposed in our group. The FUIRS employs a novel biomimetic microrobot to realize an underwater manipulation task. This paper describes the biomimetic microrobot which is inspired by an octopus. The son robot can realize basic underwater motion, i.e. grasping motion, object detection and swimming motion. To enhance the payload, a novel buoyancy force adjustment method was proposed which can provides 11.8 mN additional buoyancy force to overcome the weight of the object in water. Finally, three underwater manipulation experiments are carried out to verify the performance of the son robot. One is carried by swimming motion and buoyancy adjustment; the other two are only carried by buoyancy adjustment. And the experimental results show that the son robot can realize the underwater manipulation of different shape and size objects successfully. The swimming motion can reduce the time cost of underwater manipulation remarkably.

C. Yue (✉)
Graduate School of Engineering, Kagawa University,
2217-20, Hayashi-cho, Takamatsu, Kagawa 761-0396, Japan
e-mail: chunfengyue@gmail.com

C. Yue
College of Mechanical and Electric Engineering, Changchun
University of Science and Technology, Changchun, China

S. Guo · L. Shi
School of Life, Beijing Institute of Technology, Beijing, China

S. Guo
Faculty of Engineering, Kagawa University, 2217-20,
Hayashi-cho, Takamatsu, Kagawa 761-0396, Japan

1 Introduction

With the booming development of ocean scientific exploitation, researchers are eager to realize more and more underwater interventions by unmanned underwater vehicle. Due to the high flexibility and autonomy, AUV became to a suitable option for underwater intervention. In the University of Hawaii, Giacomo Marani et al. developed an underwater autonomous manipulator for intervention missions AUVs. This manipulator is used in a huge semi-AUV: SAUVIM, it is one of the first AUVs capable of autonomous manipulation (Marani et al. 2009; Kim and Yuh 2004). Prof. Pedro J. Sanz (University Jaume I), Pere Ridao (University of Girona) and Gabriel Oliver (Universitat de les Illes Balears) proposed a reconfigurable AUV for Intervention missions (RAUVI) which can realize underwater object searching and manipulation (http://www.irs.uji.es/rauvi/index.html; De Novi et al. 2009). They realized a simulation for intervention mission. It is suspected that the weapon used in a crime has been thrown to the sea. The mission is to find the weapon and recover it. All of these robots have same features; they used a mechanical arm to realize underwater intervention. The application of these underwater robots is tend to industrial area. The mechanical arm is heave, expensive and high payload. The robots calculated the posture and position to complete the underwater tasks (Antonelli et al. 2001; Sarkar and Podder 2001). They almost do not consider the environment effect causing by the robot, e.g. the motor noise, disturbance causing by propulsion system, however, these aspects are very important for underwater creature monitoring, and underwater manipulation for a light and irregular object.

In our lab, we proposed a micro father–son underwater intervention robotic system (FUIRS) which is used to monitor underwater creature and collect valuable object

Published online: 24 February 2015

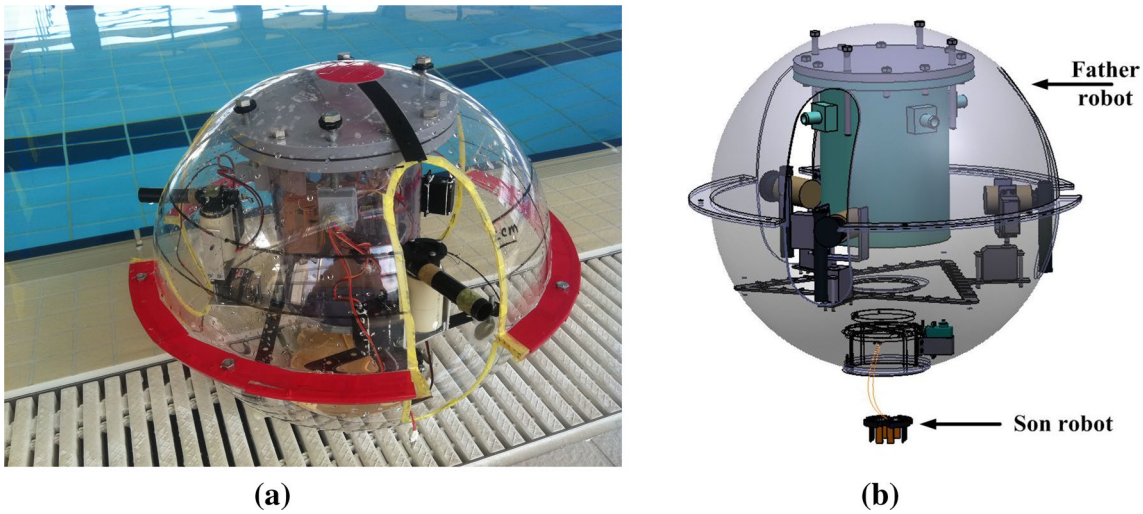

Fig. 1 The FUIRS conceptual design. **a** Prototype of the SUR-II. **b** The conceptual design of the father–son underwater intervention robotic system. The son robot can dock in the bottom of the father robot. There is a door on the bottom of the docking subsystem which is driven by a servo motor

from their living area. Different with traditional manipulation method, we employed a micro robot to instead the mechanical arm. In our previous work, we have designed and developed a spherical underwater robot (SUR-II) (Yue et al. 2012, 2013, 2014; Lin et al. 2013). Because the spherical shape and the vectored water-jet-based propulsion system, SUR-II can work in water with low noise and high stability. The conceptual design of the FUIRS is shown in Fig. 1.

As we known, nature is the best teacher. Based on the different requirements, researchers developed thousands of biomimetic robots to imitate the real creatures. Some robots can move on land, e.g. Bigdog (David Wooden et al. 2010), snake robot (Liljebäck et al. 2011), SpinybotII (Sangbae Kim et al. 2005), and so on. Some robots can fly, e.g. bug robot (Duhamel et al. 2013), bat robot (Ahmad Ghanbari et al. 2013) and SmartBird by FESTO. And some robots also can swim in water, e.g. fish robot (Yiming and Mohseni 2014; Tianjiang et al. 2014), dolphin robot (Junzhi et al. 2012), octopus-like robot (Kazakidi et al. 2012; Sfakiotakis et al. 2013) and so on. Octopus is a good hunter because it has 8 flexible arms. Based on the arms, octopus can realize swimming motion, grasping motion easily. For the son robot in FUIRS, an octopus like robot is an excellent option. First, the octopus robot can realize object manipulation by the arms. Second, it is easier to be accepted by the underwater creature rather than a high noise mechanical arm.

Ionic polymer metal composite (IPMC) is an innovative smart material which is made of an ionic polymer membrane chemically plated with gold or platinum electrode on both sides (Guo et al. 2012; Gao et al. 2011; Chang and Kim 2013). The most attractive feature of this material is no need waterproof, easy to drive, no noise, simple structure, suitable response time, high bending deformation, low drive voltage and long life (Shi et al. 2013a). This material can be designed as different shape. The high flexibility can meet the design requirements perfectly (Jain et al. 2013). The purpose of this paper is to design a son robot for the FURIS to execute underwater Intervention task, and the son robot should keep low noise and as far as possible to reduce the effect on underwater environment. To realize compact structure and low noise, IPMC actuator is adopted to drive the son robot motion.

This paper is organized as follows. The main work of Sect. 2 proposes the son robot design requirements. The main work of Sect. 3 is to invent a suitable arm for the son robot. The Sect. 4 introduces the design of the support frame and buoyancy adjustment principle. And then, the underwater experiments will be introduced in the Sect. 5 to verify the performance of the son robot. Finally, the conclusions and future work are pointed in Sect. 6.

2 Proposed son robot

Comparing with a traditional multi-function underwater vehicle-manipulator system (Farivarnejad et al. 2014), we want to realize the manipulation task by a son robot which can be delivered and recovered successfully. Considering the size and work environment of the father robot, the son robot should be small size, light weight and high flexibility. On the other hand, if a manipulator is very heavy or the payload is quite big, the motion of the manipulator

Fig. 2 The octopus grasps an object (http://www.foxnews.com/entertainment/2010). **a** Object detecting, **b** Object grasping. The overall process can be divided into 4 steps. *First*, the octopus detects the object (the football) and locks it. *Second*, the octopus swims to the top of the football and then fall on the football. Finally, the octopus grasps the football successfully

will affect the dynamical model of the vehicle. It will have the potential risk of loss the robot's balance. But for a son robot, it can realize underwater motion individually. And also, the son robot can work in a narrow space.

2.1 Inspired by an octopus

The design of the son robot is inspired by octopus, when the octopus detected an object, it will swim and fall down on the top of the target. The octopus will grasp the target with its arms. And the suckers which are placed on the arms will enhance the grasp force. The Fig. 2 shows the octopus named Paul to grasp a football.

In our research, the motion of the son robot is to imitate the octopus. 8 IPMC actuators are employed to form the arms of the son robot. One proximity sensor is used to detect the object. A custom designed frame is used to install the arm and proximity sensor. The frame is the body part of the son robot. The design detail will be introduced in the following sections.

2.2 Design requirements

Based on the discussion about father–son robotic system, the son robot must:

- Be small in size: the longest dimension less than 60 mm;
- Be light weight: less than 10 g;
- Be suitable payload: 1 g in water, 15 g in air; the maximum size is 30 × 30 × 20 mm;
- Be able buoyancy adjustment;
- Be able to realize grasping motion, floating motion in the vertical direction;
- Have the ability of object detection;
- Fit for different shape and size objects.

3 IPMC actuators for son robot arms

3.1 The electromechanical model

IPMC actuators can work in air (Jain et al. 2009) (but not absolute dry condition) and in water (Shi et al. 2013b), when the IPMC actuators work in air, the drive voltage is lower than in water because the IPMC is more easy to failure. Generally, rectangle shape is the most common options because it can generate stable deflection and bending force (Abdelnour et al. 2012). And the electromechanical model is established for the rectangle IPMC.

In order to investigate the feature of this material, (Bonomo et al. 2007) established an electromechanical model which is shown in Fig. 3. Based on this model, (Shi et al. 2012) discussed the relationship between these parameters and deflection. After taking Laplace transformation, the dynamic bending deflection of an IPMC beam $\delta\ (s)$ is determined by the concentration of water molecules $W\,(s)$ (Shi et al. 2012).

$$\delta(s) = k_v W(s) = 4k_v Q_i(s) \tag{1}$$

where k_v is the deformation coefficient of IPMC and $Q\ (s)$ is the total electric charge. Because each sodium ion takes four water molecules in the saturated state, $W\ (s) = 4Q\ (s)$. Based on Kirchoff's voltage law and (Shi et al. 2012), the deflection $\delta\ (s)$ can be expressed as (2).

$$\delta(s) = 4k_v \frac{s(R_1 + R_2)C + 1}{s^2(R_1R_2 + 2R_2R_e + 2R_1R_e)C + s(R_1 + 2R_e)} V_i(s) \tag{2}$$

where, w is the width of the IPMC actuator; h denotes the thickness of the IPMC actuator; l_c is the length of the clamped part of the IPMC actuator; l_f is the free length of the IPMC actuator. l_s is the point where the force is applied. The totally length of the IPMC actuator is $L = l_c + l_f$; δ a

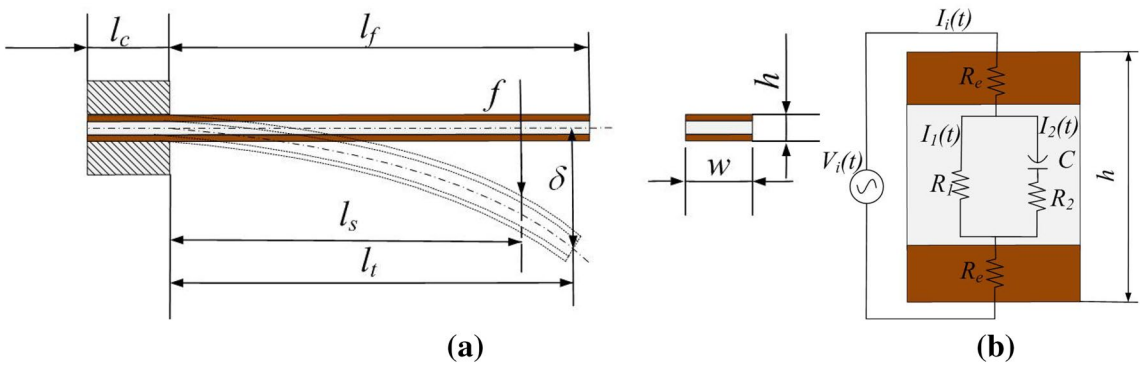

Fig. 3 **a** The mechanical configuration of the actuator. **b** The equivalent electrical circuit for an IPMC actuator (Shi et al. 2012; Bonomo et al. 2007)

is the deflection of the IPMC; f is the force applied to the IPMC sample; V_i (t) denotes the external stimulus; I_i (t) denotes the totally current across to the IPMC; $I_1(t)$ denotes the current cross R_1; I_2 (t) denotes the current cross R_2; R_e denotes the resistances of two electrodes.

3.2 The design of the arm for son robot

In (Bonomo et al. 2007), the author discussed the properties of two kinds of materials for fabricating the IPMC actuators i.e. Nation® Na^+ and Nation® Li^+. In our research, we used Nation® Na^+ to fabricate the IPMC actuator and the thickness is 0.2 mm. (Hubbard et al. 2014) fabricated the IPMC actuators with different solutions i.e. platinum complex solution and gold solution, and the author carried out a comparison experiment to investigate the difference between the two solutions. The experimental results showed that the gold solution performance a larger deflection than the platinum solution. According to the comparison results, we decided to fabricate the IPMC with gold solution.

We fabricated the IPMC in our laboratory. Because the deflection of the IPMC actuators is an essential factor for determining the dimension of the object, the bending forces and buoyancy adjustment range determine the payload, we designed the IPMC actuator after considering the design requirements. The main parameters of our IPMC actuator is $w = 8$ mm, $h = 0.22$ mm, $L = 32$ mm, $l_f = 27$ mm, and $l_c = 5$ mm.

A regular rectangle is always adopted in the related researches as mentioned in Sect. 1. But for an octopus, its arm is tapered. Usually, tapered arm is more convenient and flexible than a rectangular arm. Of course, human finger is also a perfect design for a grasping task. Considering the three ideas, we proposed 3 kinds of conceptual design for the son robot arm that is shown in Fig. 4. The Fig. 4a is a rectangular arm. The Fig. 4b is a semicircle arch that is similar to human finger. The Fig. 4c is a tapered arm.

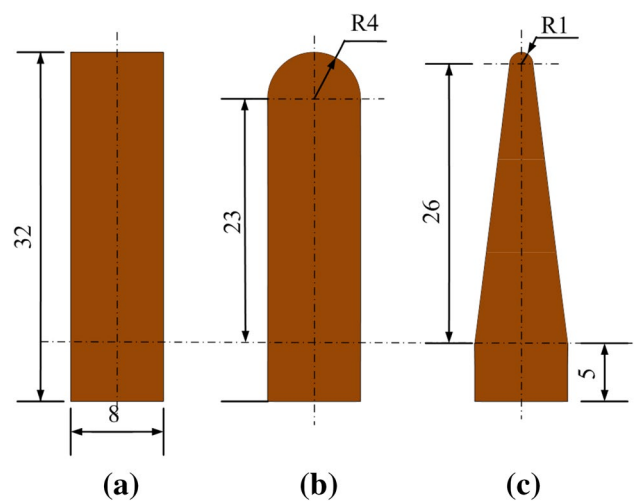

Fig. 4 Proposed conceptual design of the son robot arm. **a** Regular *rectangle*, **b** Human finger shape, **c** Octopus arm shape

3.3 The deflection and bending force test for the 3 different arms

To investigate the most suitable designing scheme, deflection test and bending force test are executed. Generally, the performance of the IPMC actuators is easily affected by the fabrication process. Therefore, the experimental results are not reliable if the experiments are carried out by different IPMC actuators. In order to get accurate and credible result, only one piece of IPMC actuator is used to carry out the test. The Fig. 5 shows the principle and experimental setup for the experiments. First, we used a regular rectangular IPMC actuator which is shown in Fig. 4a to execute the test. After getting this deflection and bending force data, we cut off the part 1 (black color) as shown in Fig. 5c. The IPMC actuator will change to a semicircle arch shape as shown in Fig. 4b. And then, we will repeat the experiment process. Finally, we cut off the part 2 (red color) as shown in Fig. 5c,

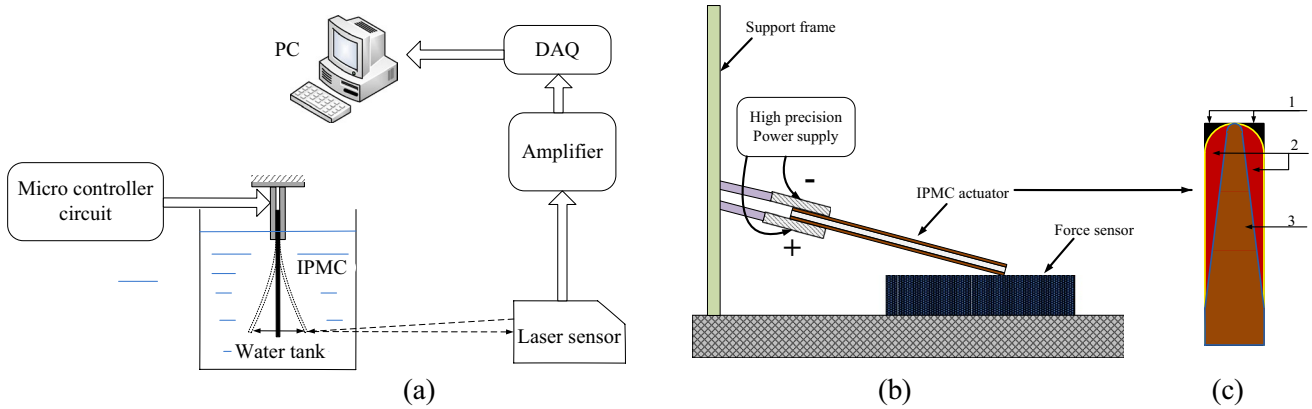

Fig. 5 Deflection and bending force experimental setup. **a** The experimental setup for deflection test. **b** The experimental setup for bending force test. **c** The process for cutting the IPMC actuator; *1–3*

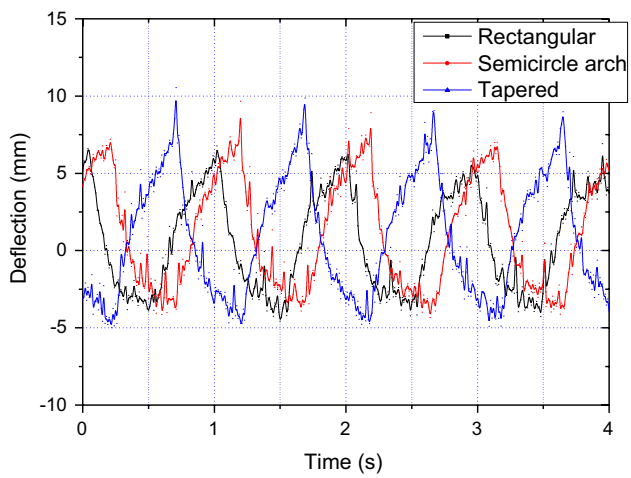

Fig. 6 The experimental results for deflection test

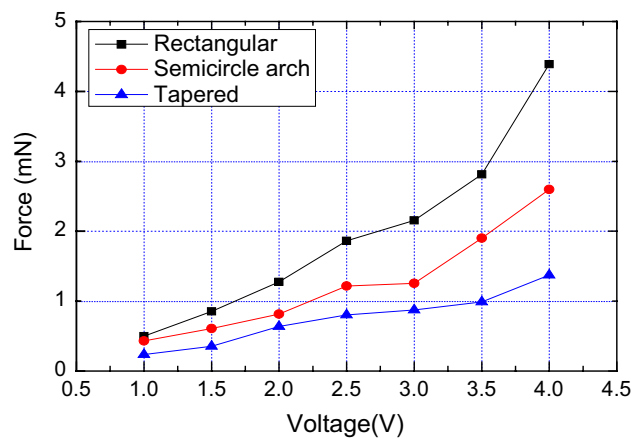

Fig. 7 The experimental results for bending force test

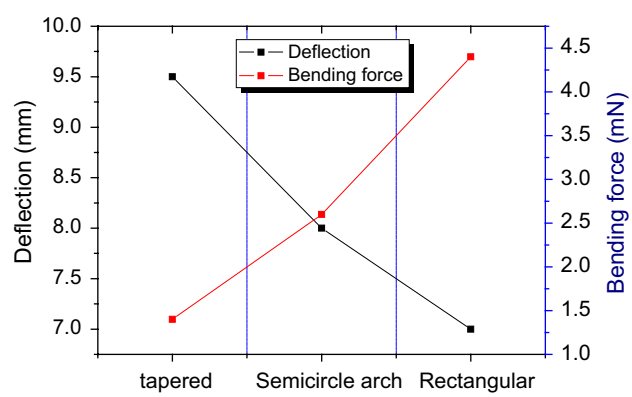

Fig. 8 The comparison result between the different shape arms

and the IPMC actuator will change to a tapered shape. We will repeat the experiment process again.

In the bending force experiment, a series voltage is acted on the IPMC respectively. Especially, there is a given angle between the IPMC and the force sensor in the bending force experiment. The tip of the IPMC contact with the force sensor, but there is no pressure. The bending force experimental results are shown in Fig. 6. In the deflection experiment, we mentioned a micro controller, it is to generate 1 Hz rectangular wave. The drive voltage is 4 V. We employ a laser sensor to detect the deflection of IPMC actuator. Due to the laser sensor is very sensitive, data calibration is necessary after changing the IPMC actuator. The deflection experimental results are shown in Fig. 7. Finally, we compared the performance of the three arms and the comparison results shows in Fig. 8.

According to the flexibility of these three kinds of arms, we tend to choose the arm which is more similar with the octopus arm. And the Fig. 6 also showed a good deflection performance for the tapered arm. However, the bending force of tapered arm is very small. The robot cannot hold the object tightly. Therefore, after compromising the above

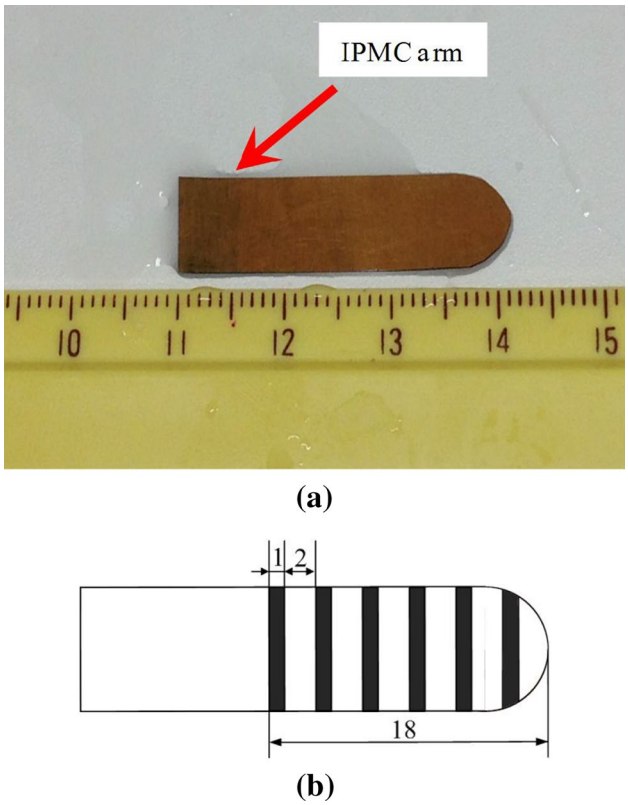

Fig. 9 **a** The prototype for the arm of the son robot. **b** The layout of the waterproof gluing (*gray part*)

factors, the semicircle arch shape is employed to form the arm. The Fig. 9a showed the prototype. Octopus depends on suckers to enhance the grasping force. For the son robot, we painted waterproof gluing on the arm to enhance the friction coefficient. To keep the bending deformation, the waterproof gluing is made as 6 equal interval rectangles which are shown in Fig. 9b.

4 Support frame for the son robot

4.1 Modeling for the support frame of the son robot

The robot is inspired by an octopus; the arms of the robot have been designed and discussed in the Sect. 3. In this session, we want to design a small support frame to install the 8 arms and a proximity sensor. The support frame should be light, and it can provide enough buoyancy force to overcome the weight of the son robot. The conceptual design is shown in Fig. 10.

In the Fig. 10, the yellow part is a cut-open view. ① is the bar for installing the IPMC arm. Totally, 8 bars are located on the side of the frame. ② is also a bar for IPMC actuator. This actuator is not for the arm, but for the buoyancy

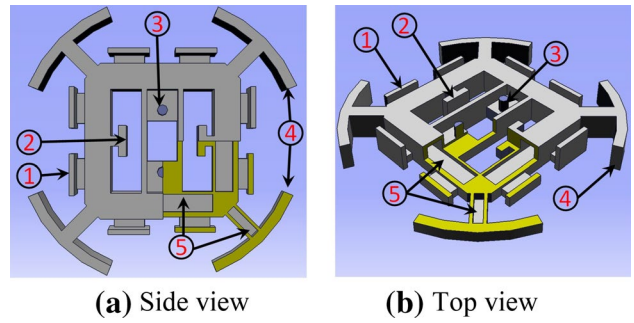

Fig. 10 The conceptual design of the support frame

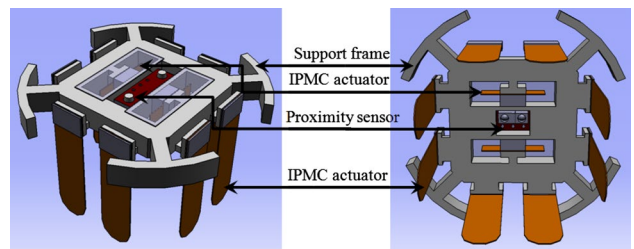

Fig. 11 The conceptual design of the assembled son robot

adjustment. ③ is for installing the proximity sensor. ④ is a beam to avoid impact from the environment. The surface hardness of IPMC is very low. Therefore, the IPMC is easy to be scratched by obstacles. The 4 beams form a circle to protect the 8 arms in horizontal direction. In order to reduce the weight and keep the buoyancy force, a series of closed rectangular grooves (No. ⑤ in Fig. 10) are designed in the frame. Due to the high complexity of the structure, 3D printing technology is used to undertake this task. And we used a low cost, hydrophobic, low density and degradable environmental protection material polylactic acid (PLA) to print the support frame.

4.2 A novel method for buoyancy adjustment

The main task of the son robot is to grasp and recover the object. To enhance the payload and recover the son robot successfully, buoyancy adjustment ability is necessary. Because the son robot is very small, there is no any commercial product can meet this requirement.

As we known, if we placed an inverted glass into a basin of water, the glass cannot completely fill with water. According to this principle, the buoyancy adjustment is proposed in Fig. 11. Two rectangular grooves are placed on the side of proximity sensor which is shown in Fig. 10a. The dimension for each groove is about $V_{gr} = 20 \times 5 \times 6\ \text{mm}^3$. Two IPMC actuators are installed in the groove respectively. We put a cover on the top of each groove to form an inverted space. The IPMC actuators also can be seen as two electrodes, and

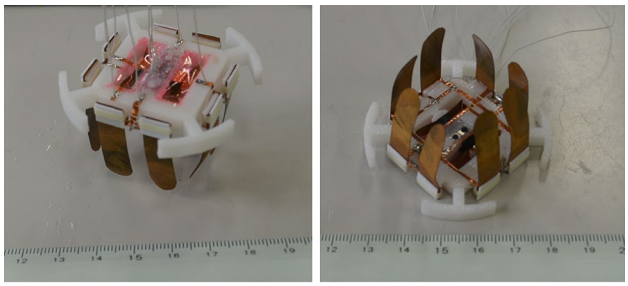

(a) Top view **(b)** Bottom view

Fig. 12 The prototype of the son robot

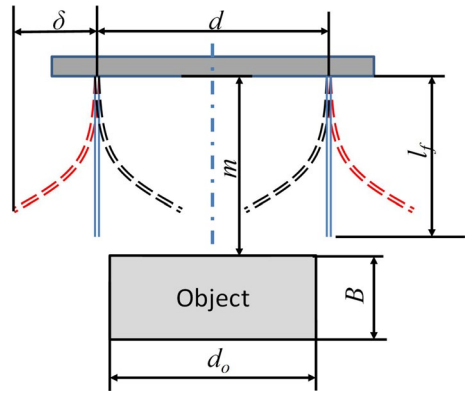

Fig. 13 The schematic diagram for the grasping motion

it can be used to electrolyze the water, forming hydrogen and oxygen gas which will fill in the grooves and provide buoyancy for the son robot (Lee et al. 2006). Based on the Archimedes law in (3), we can calculate the buoyancy that is provided by the buoyancy adjustment method.

$$F_B = \rho g V \tag{3}$$

where g is the gravity g = 9.81 m/s^2; V is volume of the hydrogen and oxygen which is collected by the grooves; ρ is the density of fluid, for water the density is ρ = 1.0 g/cm^3.

If we ignore the compression of the gas, the maximum of V_{max} is equal to the volume of the grooves.

$$V_{\max} = 2V_{gr} = 2 \times 20 \times 5 \times 6 = 1200\,\text{mm}^3 \tag{4}$$

And we can obtain the maximum buoyancy force is $F_{Bmax} = 11.8$ mN. The prototype of the son robot is shown in Fig. 12.

4.3 Discussion for the grasping motion and swimming motion

The eight arms of the son robot form a cubic area to hold the object which is shown in Figs. 11, 12, when the son robot approaches the object, the arms will be opened to increase the successful probability of grasping motion. The grasping motion is shown in Fig. 13. The red line stands for the opened state, the black line stands for the closed state, and the blue line stand for the normal state.

Where, $n = d + 2\delta$ is the maximum range for the son robot; d_0 is the dimension of the object; $d = 36$ mm is the distance between the two arms; δ is the deformation for the arm, and the maximum value can reach to 15 mm; m is the distance between the object and the son robot. The dimension of the object should satisfy the (5).

$$\begin{cases} c(d - 2\delta) < d_0 < d \\ B < l_f \end{cases} \tag{5}$$

where, c is a constant, it is to ensure the object can be held tightly, $1 < c < d/(d\text{-}2\delta)$.

Table 1 The main features of the son robot

Feature	Son robot
Dimension (mm)	φ50 × 32
Weight (g)	6.1
Range[a] (mm)	d_0:9 ~ 36, B: 10 ~ 27
Payload (g)	1.0
Actuator quantity	10

[a] The dimension range of the objects for underwater manipulation

Based on the (5), the dimension of the object should be; $6c < d_0 < 36$ mm, and we defined the c = 1.5, therefore, 9 mm < d_0 < 36 mm. The main feature of the son robot is shown in Table 1.

This son robot also can flap arms to realize swimming motion, and the swimming motion can overcome a part of payload for the manipulation task.

5 The manipulation experiments for the son robot

5.1 Manipulation experimental process and results

As mentioned in the design requirements, this robot is not only designed for a specific object. We also want it to fit for a various different objects. Therefore, 3 typical shapes are selected in these experiments, i.e. cuboid, cylinder and sphere. The prototype of the 3 objects is shown in Fig. 14. To test the payload of the son robot and the dimension range of the objects, the 3 objects are different in weight and dimension. The detail information of the objects is shown in Table 2.

In these experiments, we assume that the father robot have detected the object and hovering on the top of the object. The launching system which is shown in Fig. 15 stands for the father robot. The experiment is executed in a 25 cm × 50 cm water tank. The experimental condition as

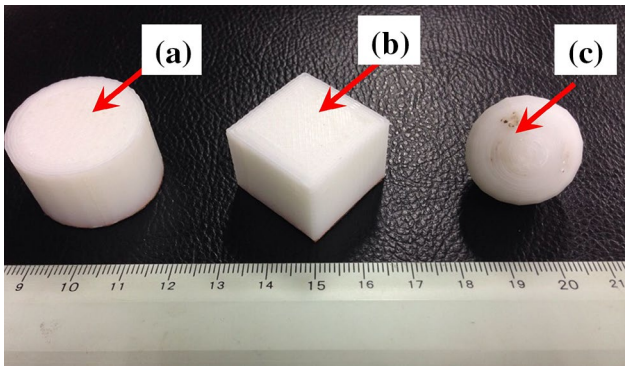

Fig. 14 The objects for underwater manipulation experiments, **a** is a *cylinder*, **b** is a *cuboid* and **c** is a *sphere*

Table 2 The main feature of the Objects

Feature	Manipulation objects		
	Cylinder	Cuboid	Sphere
Dimension (mm)	φ30 × 18	25 × 25 × 18	R = 12
Weight in air (g)	13.74	12.15	7.82
Weight in water (g)	1.02	0.9	0.58

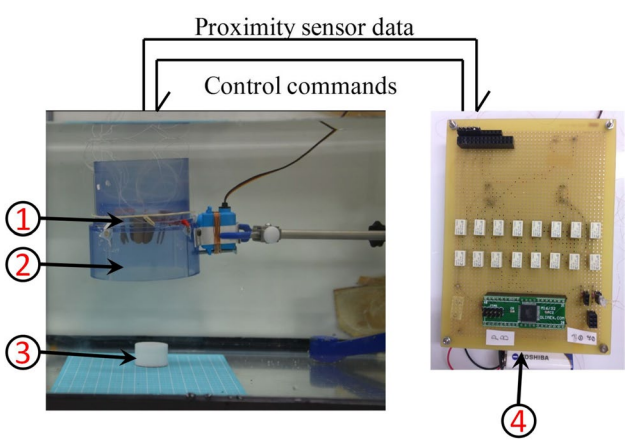

Fig. 15 The experimental setup. Where, ① is the son robot; ② is the launching structure; ③ is the object for manipulation experiment; ④ is the control circuit for the son robot

follows: still water; water depth: 30 cm; manipulation distance: 15 cm; temperature: 25 °C.

The experimental process as follows:

(a) The son robot is activated by the father robot (power on);
(b) The launching system delivery the son robot;
(c) The son robot opens the arms and detects the object by the proximity sensor;
(d) After the son robot detected the object, the robot grasps it tightly and triggers the buoyancy adjustment;

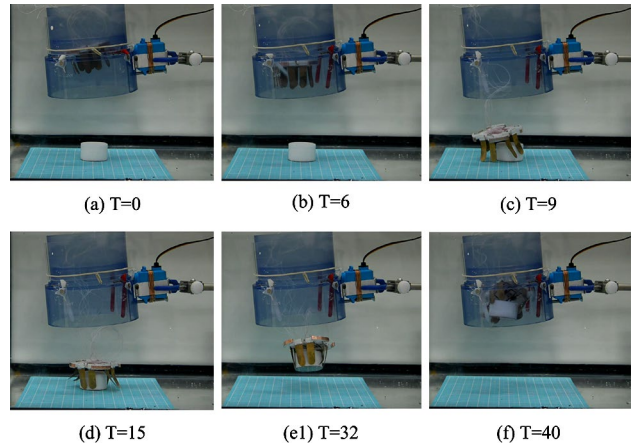

Fig. 16 The snapshot of the experiment for the *cylindrical* object

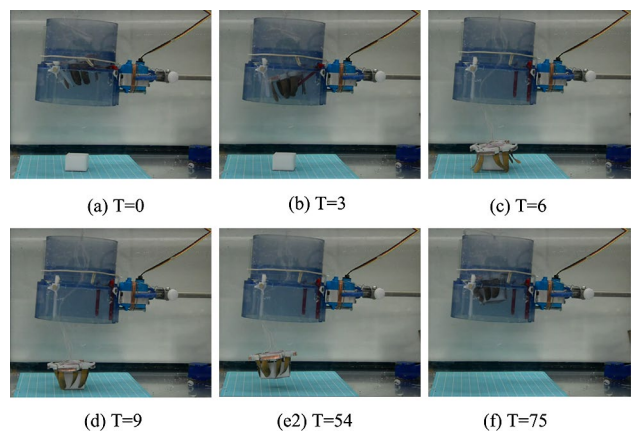

Fig. 17 The snapshot of the experiment for the *rectangular* object

(e1) The two half open grooves collected gas. The robot uses 4 arms to grasp the object and 4 arms to swim;
(e2, e3) After the two half open grooves collected enough gas, the robot will float up;
(f) The robot will go back to the launching system.

The experimental setup is shown in Fig. 15. And the experimental results are shown in Figs. 16, 17 and 18.

5.2 Discussion for the experimental results

In the three experiments, the son robot completed the task successfully. But, there still some problems should be discussed in detail. We compared the time cost in the Fig. 19. In the experiment for cylindrical object, the time cost is less than 20 s for each step, because the swimming motion reduced the time cost markedly. But in the experiments for rectangular and spherical object, there is a long time cost in step (e). The time cost is for buoyancy adjustment. Second,

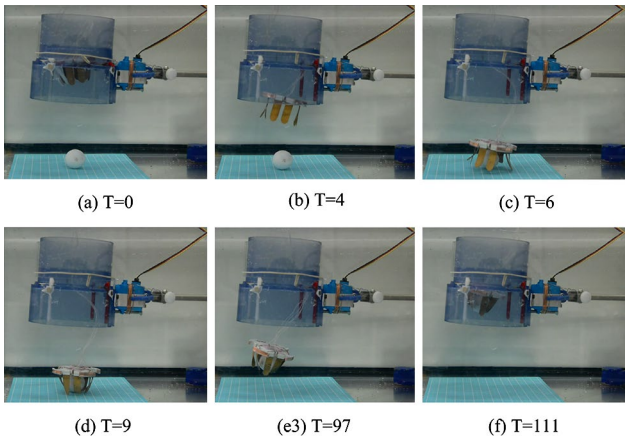

Fig. 18 The snapshot of the experiment for the *spherical* object

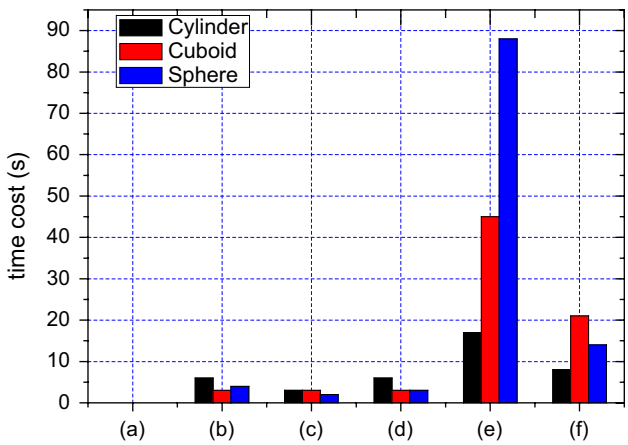

Fig. 19 Time cost for the each step of the underwater manipulation

after grasping the object, the son robot floats up and go back to the launching system by itself. However, it is very difficult to realize because the turbulence is always happening. Third, the feasibility of these experiments depends on the precision of the father robot and the flow field situation. Finally, this robot only can realize underwater motion in 1 degree of freedom.

6 Conclusions and future work

This paper presents a son robot for the father–son underwater intervention robotic system (FUIRS) which is inspired by octopus motion. The IPMC smart material is adopted to form the arm of son robot. We have designed the son and discussed the features of the actuator. A novel buoyancy adjustment method is proposed to enhance the load capacity and reduce the time cost for underwater manipulation. The maximum buoyancy force is about 11.8 mN. Finally, we have carried out three underwater manipulation experiments for three different objects. The experimental results show that the robot can fit for different shape and size objects and the son robot can realize underwater manipulation successfully. Meanwhile, based on the swimming motion, the son robot can reduce the time cost remarkably.

In the future, to enhance the flexibility of the son robot, wireless method is considering driving the son robot. We also want to test some more difficult objects e.g. a cone. And how to improve the buoyancy adjustment method should be considered. A closed-loop control in horizontal direction is necessary to enhance the performance of the son robot.

Acknowledgments This research project is partly supported by National Natural Science Foundation of China (61375094), and Key Research Program of the Natural Science Foundation of Tianjin (13JCZDJC26200).

References

Abdelnour K, Stinchcombe A, Porfiri M, Zhang J, Childress S (2012) Wireless powering of ionic polymer metal composites toward hovering microswimmers. IEEE/ASME Trans Mechatron 17:924–935

Antonelli G, Chiaverini S, Sarkar N (2001) External force control for underwater vehicle-manipulator systems. IEEE Trans Robot Autom 17:931–938

Bonomo C, Fortuna L, Giannone P, Graziani S, Strazzeri S (2007) A nonlinear model for ionic polymer metal composites as actuators. J Smart Mater Struct 16:1–12

Chang Y, Kim W (2013) Aquatic ionic-polymer-metal-composite insectile robot with multi-DOF legs. IEEE/ASME Trans Mechatron 18:547–555

De Novi G, Melehiorri C, Garcia JC, Saoz PJ, Rldao P, Oliver G (2009) A new approach for a reconfigurable autonomous underwater vehicle for intervention systems conference, 2009 3rd Annual IEEE, Vancouver, pp 23–26, 23–26 March 2009

Duhamel P-EJ, Pérez-Arancibia NO, Barrows GL, Wood RJ (2013) Biologically inspired optical-flow sensing for altitude control of flapping-wing microrobots. IEEE/ASME Trans Mechatron 18:556–568

Farivarnejad H, Ali S, Moosavian A (2014) Multiple impedance control for object manipulation by a dual arm underwater vehicle–manipulator system. Ocean Eng 89:82–98

Gao B, Guo S, Ye X (2011) Motion-control analysis of ICPF-actuated underwater biomimetic microrobots. Int J Mechatron Autom 1:79–89

Ghanbari A, Mottaghi E, Qaredaghi E (2013) A new model of bio-inspired bat robot. In: Proceeding of the 2013 RSI/ISM international conference on robotics and mechatronics, Tehran, pp 403–406, 13–15 Feb 2013

Guo S, Shi L, Xiao N, Asaka K (2012) A biomimetic underwater microrobot with multifunctional locomotion. Robot Autom Syst 60:1472–1483

http://www.foxnews.com/entertainment/2010/10/26/paul-octopus-world-cup-oracle-dies/

http://www.irs.uji.es/rauvi/index.html

Hubbard JJ, Fleming M, Palmre V, Pugal D, Kim KJ, Leang KK (2014) Monolithic IPMC fins for propulsion and maneuvering in bioinspired underwater robotics. IEEE J Ocean Eng 39:540–551

Hu T, Low KH, Shen L, Xu X (2014) Effective phase tracking for bioinspired undulations of robotic fish models: a learning control approach. IEEE/ASME Trans Mechatron 19:191–200

Jain RK, Parkar US, Majumdar S (2009) Micro gripper for micromanipulation using IPMCs (ionic polymer metal composites). J Sci Ind Res 68:23–28

Jain RK, Majumder S, Dutta A (2013) SCARA based peg-in-hole assembly using compliant IPMC micro gripper. Robot Auton Syst 61:297–311

Yu J, Su Z, Wang M, Tan M, Zhang J (2012) Control of yaw and pitch maneuvers of a multilink dolphin robot. IEEE Trans Robot 28:318–329

Kazakidi A, Vavourakis V, Pateromichelakis N, Ekaterinaris JA, Tsakiris DP (2012) Hydrodynamic analysis of octopus-like robotic arms 2012 IEEE international conference on robotics and automation, St Paul, USA, pp 5295–5300, 14–18 May 2012

Kim TW, Yuh J (2004) Development of a real-time control architecture for a semi-autonomous underwater vehicle for intervention missions. Control Eng Pract 12:1521–1530

Kim S, Asbeck AT, Cutkosky MR, Provancher WR (2005) SpinybotII: climbing hard walls with compliant microspines, advanced robotics, 2005. ICAR'05. In: Proceedings 12th international conference on, Seattle, pp 601–606, 18–20 July 2005

Lee J-W, Vinh KN, Park S-Y, Yoo Y-T (2006) Electrolytic stability of various inner solutions in an ionic polymer metal composite. J Korean Phys Soc 48:1594–1600

Liljebäck P, Pettersen KY, Stavdahl Ø, Gravdahl JT (2011) Controllability and stability analysis of planar snake robot locomotion. IEEE Trans Autom Control 56:1365–1380

Lin X, Guo S, Yue C, Du J (2013) 3D modelling of a vectored water jet-based multi-propeller propulsion system for a spherical underwater robot. Int J Adv Rob Syst. doi:10.5772/51537

Marani G, Choi SK, Yuh J (2009) Underwater autonomous manipulation for intervention missions AUVs. Ocean Eng 36:15–23

Sfakiotakis M, Kazakidi A, Pateromichelakis N, Tsakiris DP (2013) Octopus-inspired eight-arm robotic swimming by szculling movements 2013 IEEE international conference on robotics and automation, Karlsruhe, German, pp 5155–5161, 6–10 May 2013

Sarkar N, Podder TK (2001) Coordinated motion planning and control of autonomous underwater vehicle-manipulator systems subject to drag optimization. IEEE J Ocean Eng 26:228–239

Shi L, Guo S, Kudo H, Asaka K (2012) Development of a venus flytrap-inspired robotic flytrap. In: Proceeding of the 2012 IEEE international conference on robotics and biomimetics, Guangzhou, pp 551–556, 11–14 December 2012

Shi L, Guo S, Mao S, Li M, Asaka K (2013a) Development of a lobster-inspired underwater microrobot. Int J Adv Rob Syst. doi:10.5772/54868

Shi L, Guo S, Pan S, He Y, Guo P (2013b) A multifunctional underwater microrobot for mother–son underwater robot system. In: Proceeding of the IEEE international conference on robotics and biomimetics, Shenzhen, pp 1007–1012, 12–14 December 2013

Wooden D, Malchano M, Blankespoor K, Howard A, Rizzi AA, Raibert M (2010) Autonomous navigation for bigdog 2010 IEEE international conference on robotics and automation, Anchorage, Alaska, pp 4736–4741, May 3–8, 2010

Xu Y, Mohseni K (2014) Bioinspired hydrodynamic force feedforward for autonomous underwater vehicle control. IEEE/ASME Trans Mechatron 19:1127–1137

Yue C, Guo S, Lin X, Du J (2012) Analysis and improvement of the water-jet propulsion system of a spherical underwater robot. In: Proceedings of 2012 IEEE international conference on mechatronics and automation, Chengdu, pp 2208–2213, 5–8 August 2012

Yue C, Guo S, Shi L (2013) Hydrodynamic analysis of a spherical underwater robot: SUR-II. Int J Adv Rob Syst. doi:10.5772/56524

Yue C, Guo S, Li Y, Li M (2014) Bio-inspired robot launching system for a mother–son underwater manipulation task. In: Proceedings of 2014 IEEE international conference on mechatronics and automation, Tianjin, pp 174–179, 3–6 August 2014